Freshwater Biology (2007) **52,** 680–695 doi:10.1111/j.1365-2427.2007.01726.x

Stream ecosystem responses to spatially variable land cover: an empirically based model for developing riparian restoration strategies

THOMAS E. JOHNSON,* JAMES N. MCNAIR,* PUNEET SRIVASTAVA† AND DAVID D. HART‡
*Patrick Center for Environmental Research, Academy of Natural Sciences of Philadelphia, Philadelphia, PA, U.S.A.
†Biosystems Engineering Department, Auburn University, Auburn, AL, U.S.A.
‡Senator George J. Mitchell Center for Environmental and Watershed Research, University of Maine, Orono, ME, U.S.A.

SUMMARY

1. The restoration of native, forested riparian habitats is a widely accepted method for improving degraded streams. Little is known, however, about how the width, extent and continuity of forested vegetation along stream networks affect stream ecosystems.
2. To increase the likelihood of achieving restoration goals, restoration practitioners require quantitative tools to guide the development of restoration strategies in different catchment settings. We present an empirically based model that establishes a relationship between a 'stress' imposed at different locations along a stream by the spatial pattern of land cover within catchments, and the response of biologically determined ecosystem characteristics to this stress. The model provides a spatially explicit, quantitative framework for predicting the effects of changes in catchment land cover composition and spatial configuration on specific characteristics of stream ecosystems.
3. We used geospatial datasets and biological data for attached algae and benthic macroinvertebrates in streams to estimate model parameters for 40 sites in 33 distinct catchments within the mid-Atlantic Piedmont region of the eastern U.S. Model parameters were estimated using a genetic optimisation algorithm. R^2 values for the resulting relationships between catchment land cover and biological characteristics of streams were substantially improved over R^2 values for spatially aggregated regression models based on whole-catchment land cover.
4. Using model parameters estimated for the mid-Atlantic Piedmont, we show how the model can be used to guide restoration planning in a case study of a small catchment. The model predicts the quantitative change in biological characteristics of the stream, such as indices of species diversity and species composition, that would occur with the implementation of a hypothetical restoration project.

Keywords: land cover, land use, management tool, mid-Atlantic, model, Piedmont, planning, prioritisation, restoration, riparian, stream ecosystem

Introduction

Streams are tightly connected to their catchments through the lateral and longitudinal transport of materials derived from terrestrial habitats (Hynes, 1975; Montgomery & Buffington, 1993; Allan, 2004). Upland areas contribute materials such as sediment and nutrients to streams by downslope hydrologic transport. Streams are also internally connected by fluvial transport processes, with downstream locations being strongly influenced by upstream locations (Allan, 1995; Gomi, Sidle & Richardson, 2002; Ward *et al*., 2002).

Correspondence: Thomas E. Johnson, U.S. EPA NCEA, 1200 Pennsylvania Ave. NW, Washington DC, 20460, U.S.A. E-mail: johnson.thomas@epa.gov

Throughout the U.S., many catchments have been impacted by the conversion of native vegetation to agriculture and urban/suburban (hereafter, urban) development. In the mid-Atlantic U.S., most catchments now occur as spatially diverse mosaics of different land-cover types variously affected by human use. In these areas, land cover conversion has substantially altered the character and quantity of landscape-derived materials transported to streams resulting in degraded water quality and instream habitat, and impaired biological communities.

Riparian habitats are particularly important to stream ecosystems, yet have been substantially affected by land cover conversion [Gregory *et al.*, 1991; Welsch, 1991; National Research Council (NRC), 2002]. Riparian habitats influence not only the downslope hydrologic transport of materials (Sweeney, 1992; Correll, 2000; Gove, Edwards & Conquest, 2001), but also processes such as shading by trees (which reduces energy inputs of sunlight and heat), and input of leaves, woody debris and other materials during high-flow events that inundate the floodplain (Junk, Bayley & Sparks, 1989; Tabacchi *et al.*, 1998; Amoros & Bornette, 2002).

In catchments where riparian habitats have been disturbed, riparian restoration is widely accepted as a method for improving degraded stream ecosystems (NRC, 2002; Bernhardt *et al.*, 2005). In the eastern U.S., restoration typically involves the re-establishment of native, riparian forest land cover. The outcomes of individual projects are not well understood, however, and are likely to vary in different catchment settings. Restoration planning should account for processes operating across multiple spatial scales within catchments (Bell, Fonseca & Motten, 1997; Wissmar & Beschta, 1998; Bohn & Kershner, 2002), but project siting often occurs opportunistically based on local factors such as landowner cooperation. Furthermore, little is known regarding the dependence of specific stream ecosystem attributes on structural properties such as the width, extent and continuity of forested riparian habitat within a stream network (Moser *et al.*, 2000). It is therefore likely that riparian restoration is being implemented in a sub-optimal way, especially when the goal is to improve in stream ecological conditions.

To increase the likelihood of achieving restoration goals, restoration practitioners require planning tools that can be applied at the catchment scale to make quantitative predictions of project outcomes. To date, however, no fully satisfactory modelling tool has emerged, although several useful approaches have been developed.

Hillslope-scale mechanistic models have been developed that are capable of predicting how the width and composition of riparian habitats influence material loadings to streams. An example is the Riparian Ecosystem Management Model (REMM; Lowrance *et al.*, 2000; Altier *et al.*, 2002), which can be used to predict the effect of riparian buffers on stream chemistry when loadings of sediment and nutrients to the riparian zone are known. Like other mechanistic models, application of REMM is limited by its complexity and large requirements for input data. It also operates at the hillslope rather than catchment scale, and does not predict effects on instream ecological endpoints.

Empirical models provide an alternative approach. Numerous studies suggest that when appropriate scales are considered, the type and pattern of catchment land use can be used to indicate a range of instream ecosystem characteristics (e.g. Jones *et al.*, 2001; Sponseller, Benfield & Valett, 2001; Strayer *et al.*, 2003). Empirically derived relationships thus appear to provide information useful to guide restoration planning. Application of empirical models requires a spatially explicit approach, however, rather than the more common models based on spatially aggregated land cover metrics. For example, the concept of spatially referenced regression utilised in the USGS SPARROW model provides a framework that could be adapted to guide restoration planning based on projected project outcomes (Smith, Schwarz & Alexander, 1997; Preston & Brakebill, 1999).

In this paper, we develop an empirically based, spatially explicit model that establishes a relationship between the 'stress' imposed at any stream location by catchment land cover (e.g. due to sediment and nutrient loads generated) and the response of biological ecosystem properties to this stress. We then illustrate how the model could be used to guide restoration planning in a case study catchment in the mid-Atlantic Piedmont region of the eastern U.S. Model parameters are estimated using land cover and biological data for streams in 33 small catchments, and the model is used to estimate the change in biological characteristics of the stream that would result from implementing a hypothetical restoration project.

Model development

The model we develop combines elements of spatially distributed hydrologic models, spatially referenced regression models, and ecological risk assessment. It is designed to have manageable data requirements, a relatively small number of parameters, and a level of mechanistic detail that is high enough so parameters have reasonably clear interpretations, but low enough so the model remains transparent to the principles underlying its behaviour. This section outlines the conceptual basis of the model and develops the model equations.

Conceptual framework

The conceptual basis of the model consists of four key ideas:

1 Each spatial unit (grid cell) of a catchment acts as a source of land cover-related materials and energy that are transported along hillslope pathways to a stream, where they act as stressors on the stream ecosystem.

2 The stressor loading from each grid cell declines during downslope and downstream transport, with the attenuation rate depending on land-cover types and stream properties (e.g. stream order) encountered along the transport route.

3 The level of stress that the stream ecosystem experiences at any given location is determined by the cumulative residual (non-attenuated) stressor loads contributed by all upstream/upslope grid cells.

4 The condition or integrity of the stream ecosystem at any given location is determined by the cumulative stressor load at that location and a stressor–response function that maps stressor load (or concentration) to ecosystem integrity.

Thus, catchment land cover contributes materials and energy to the stream which, together with their longitudinal rate of instream loss or dilution, determine the cumulative stressor load to which the stream ecosystem at any point is subject. This cumulative stressor load then determines stream ecosystem integrity via a stressor–response function.

In this context, a stressor is assumed to be any material or form of energy (e.g. light or heat) entering the stream that is capable of producing a negative ecological impact, whether through an increase (e.g. increased nutrient loading resulting in excessive algal growth) or decrease (e.g. decreased loadings of leaf litter and large woody debris that reduce food or habitat for benthic macroinvertebrates) relative to an appropriate reference condition. The level of stress thus refers to the magnitude of change in stressor load or concentration relative to the reference. Stressor attenuation during transport results from various processes of uptake, adsorption, decay, or transformation (e.g. photolysis or biotransformation of chemical compounds), and filtering.

Conceptually similar approaches have been used to model material loading to streams (Smith *et al*., 1997; Preston & Brakebill, 1999; Endreny & Wood, 2003) and to describe the retention of materials derived from upslope locations by forested riparian buffers (Weller, Jordan & Correll, 1998). We take the additional step of relating predicted levels of instream stress to stream ecological integrity using the concept of a stressor–response function from ecological risk assessment. Stressor–response relationships describe in a simple way the complex processes that determine how stream ecosystems respond to stress [e.g. U.S. Environmental Protection Agency (EPA), 1998]. The functional forms of stressor–response relationships between land cover and stream ecosystem characteristics are not well known, but non-linear forms are likely for impacts on biological attributes (Dale-Jones *et al*., 1999; Harris, 2002; Yuan & Norton, 2003).

Basic equations

In this section we translate the conceptual framework presented previously into a suitable set of equations. Equations are developed in a discrete form that provide a basis for applying the model to real catchments using a raster geographical information system (GIS).

Assumptions and notation. Let the catchment be divided into discrete subunits, or grid cells, labelled 1, 2, …, N. In practice, these grid cells typically will be arranged in a rectangular array, with cell size determined by the resolution of the spatial data being used. Each grid cell can be either terrestrial or aquatic. To simplify the present exposition, we assume all aquatic grid cells lie in streams, and we assume that streams are one grid cell wide. Associated with each grid cell, we assume there is an elevation and a land-cover type. We assume there is a finite collection of land-cover types, denoted t_1, t_2, …, t_K. To reduce the complexity of model notation, we include stream characteristics among these land-cover types. For example, terrestrial land-cover types might include forest, meadow, agriculture, and urban, while stream land-cover types might include first-, second-, and third-order streams.

Associated with each land-cover type, we assume there is an initial stressor loading (possibly zero) and an exponential stressor attenuation rate. The stressor loading rate represents the amount of stressor generated within a grid cell per unit time (e.g. mass per year). The stressor attenuation rate represents the exponential rate, per unit distance, at which the stressor load is attenuated during transport through a grid cell. To simplify the present exposition, we assume there is a single dominant stressor, but the model can easily be extended to address multiple stressors. Similarly, the model can be extended to allow factors other than land cover (e.g. soil properties and management practices) to influence stressor loadings and attenuation rates.

Let T be a generic symbol denoting the land-cover type of a grid cell (with possible values t_1, t_2, …, t_K). Then under our assumptions, the stressor loading from a grid cell is simply a function of T, which we will call $\lambda(T)$. Similarly, the stressor attenuation rate of a grid cell is simply a function of T, which we will call $\alpha(T)$. The proportion of transported stressor that is *not* attenuated, or lost, during transit through a grid cell is therefore given by $\exp[-\alpha(T)d]$, where d is the transport distance through the cell.

We assume that for each grid cell, there is a unique hydrologic flowpath that connects it to the catchment outlet. Each flowpath is assumed to consist of a sequence of straight line segments connecting the midpoints of neighbouring grid cells. Thus, if grid cells i, j and k are three consecutive cells along a flowpath, the portion of the flowpath lying within cell j has two components: the second half of the segment connecting cells i and j, and the first half of the segment connecting cells j and k. In practice, flowpaths can be estimated using GIS software to determine the direction of steepest descent from each grid cell, based on cell elevation and the distance between midpoints of neighbouring cells. Thus, starting from a particular grid cell, the next grid cell along the flowpath will be the neighbouring cell for which the slope between cell midpoints is negative and greatest in absolute value (unless there is no such single cell, in which case additional criteria must be employed, as in the FLOWDIRECTION function of ArcGIS).

Land cover-derived stressor loadings and the terrestrial phase of transport. Consider a representative terrestrial grid cell i. The hydrologic flowpath connecting cell i to the catchment outlet will have two parts: an initial terrestrial part and a subsequent aquatic (instream) part. We are first concerned with the terrestrial part.

Let us label consecutive cells along the terrestrial part of the flowpath from cell i $(i, 0)$, $(i, 1)$, $(i, 2)$, $\cdots$, (i, m_i), where $(i, 0)$ is grid cell i and (i, m_i) is the last cell on the terrestrial part of the flowpath and therefore borders the stream. Let the first instream cell along the flowpath be labelled $(i, m_i{+}1)$, to which it will be convenient to give the special name s_i. Let T_{ij} denote the land-cover type of flowpath cell (i, j), with possible values $t_1, t_2, \cdots, t_K$. Cell $(i, 0)$ contributes loading $\lambda(T_{i0})$, which is transported along the flowpath. (We will follow the convention of assuming that $\lambda(T_{i0})$ is the *net* loading from cell i after accounting for within-cell attenuation of the gross loading.) Attenuation processes within each grid cell along the flowpath reduce the transported load. Under our assumptions, the proportion of the load entering cell (i, j) that survives attenuation and is transported to cell $(i, j + 1)$ is $\exp(-\alpha(T_{ij})d_{ij})$, where d_{ij} is the transport distance through cell (i, j). The proportion surviving attenuation through m consecutive cells is simply the product of the survival proportions in the various cells. The residual load from cell i that reaches the stream and enters cell s_i, denoted $\rho(i \to s_i)$, is therefore given by

$$\rho(i \to s_i) = \lambda(T_{i0})\mathrm{e}^{-\sum_{j=1}^{m_i} \alpha(T_{ij})d_{ij}}. \quad (1)$$

We can simplify this expression somewhat by noting that each land cover T_{ij} must be one of the types t_1, t_2, …, t_K, and (under our assumptions) every grid cell with the same land-cover type will have the same attenuation rate. Thus, the residual load reaching instream cell s_i from terrestrial cell i can also be expressed as

$$\rho(i \to s_i) = \lambda(T_{i0})\mathrm{e}^{-\sum_{k=1}^{K} \alpha(t_k)d(t_k; i \to s_i)}, \quad (2)$$

where the summation is now over land-cover types rather than flowpath cells. Here, $d(t_k;\, i \to s_i)$ denotes the cumulative transport distance through cells along the flowpath between i and s_i (excluding i and s_i) whose land-cover type is t_k; that is,

$$d(t_k; i \to s_i) = \sum_{j:T_{ij}=t_k, 0<j<s_i} d_{ij}. \tag{3}$$

Stressor loadings to a stream and the aquatic phase of transport. The stressor load contributed by grid cell i to the stream is subsequently routed downstream, essentially as we did for the terrestrial portion of the flowpath. We again must take into account the rate (per unit distance) of attenuation during transport, which may vary along a stream with properties such as discharge and current velocity (Stream Solute Workshop, 1990; Alexander, Smith & Schwarz, 2000). Let the grid cells on the instream portion of the flowpath be labelled (i, m_i+1), (i, m_i+2), …, (i, n_i), where cell (i, n_i) is the catchment outlet or other stream location of interest, to which it will be convenient to give the special name x (the same for all grid cells in the catchment). As we have included stream properties among the land-cover types t_1, t_2, …, t_K, we can immediately extend eqn (1) to include the entire flowpath from i to x. The residual load reaching cell (i, n_i) is therefore given by

$$\rho(i \to x) = \lambda(T_{i0})\mathrm{e}^{-\sum_{j=1}^{n_i-1} \alpha(T_{ij})d_{ij}}. \tag{4}$$

Similarly, eqn (2) becomes

$$\rho(i \to x) = \lambda(T_{i0})\mathrm{e}^{-\sum_{k=1}^{K} \alpha(t_k)d(t_k; i \to x)}. \tag{5}$$

Cumulative stress at a stream location. We have routed the stressor load contributed by representative grid cell i downslope to the stream, which it enters at cell s_i, and then downstream to the catchment outlet at cell x. But grid cell i is not the only cell whose residual load reaches cell x. The cumulative stressor load in cell x, denoted $\rho(x)$, is the sum of the residual stressor loads from all grid cells whose flowpaths pass through x. That is,

$$\rho(x) = \sum_{i=1}^{N} \rho(i \to x), \tag{6}$$

We assume that impacts on stream ecosystem integrity at x are the result of exposure to this cumulative load.

Before proceeding, we note that the instream stressor level has thus far been quantified by a mass load. However, for certain stressors and biological endpoints, it may be more reasonable to quantify this level using an instream concentration, as when addressing impacts of elevated nutrients on algal growth. To do this, the stressor loading (e.g. mass per year) from each flowpath to the grid cell where it enters the stream is simply divided by stream flow through that cell (e.g. volume per year), yielding an average concentration.

Ecological integrity and the stressor–response function. Equation (6) expresses the dependence of cumulative stress at a particular stream location on land cover-related stressor loadings and attenuation rates throughout the catchment. To complete the model, we need an appropriate form of stressor–response function that expresses the dependence of stream integrity on the cumulative stressor load. In this context, stream integrity can refer to any representative measure of the reach-scale condition of stream ecosystems (Barbour *et al.*, 1999). Ideally, integrity should be quantified by an index that collapses multivariate data on the composition of biological assemblages into a single number per sample. Common examples include diatom species diversity, the Hilsenhoff Biotic Index (HBI) for benthic macroinvertebrates, and the Index of Biotic Integrity for fish (Barbour *et al.*, 1999). Application of the model assumes that an appropriate index has been selected, but is not tied to use of a particular index.

We assume that stream integrity $I(x)$ at any location x is a function of the cumulative stressor load $\rho(x)$. Thus,

$$I(x) = f(\rho(x)), \tag{7}$$

where $f(\rho)$ is the stressor–response function. (Note: stream integrity also depends on factors that are not driven by land cover in the catchment and that therefore are not reflected in the cumulative stressor load; in the current version of the model, we assume these other factors are approximately constant across the streams to which the model is being applied.) For many anthropogenic stressors, it is likely that stream integrity will be greatest when the stressor is absent ($\rho = 0$) and will decrease with increasing stress loads, as shown in the examples of Fig. 1. For other stressors,

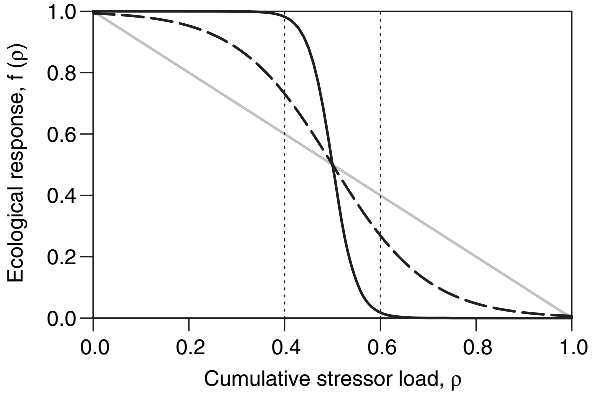

Fig. 1 Three examples of stressor–response functions. Grey curve: linear stressor–response function. Dashed and solid curves: non-linear (sigmoid) stressor–response functions. The vertical dotted lines mark the approximate range of sensitivity to changes in cumulative stressor load for the solid curve; outside this range, changes in the stressor load produce little change in response.

however, stream integrity will be greatest when the stressor is present at some level $\rho_1 > 0$ and will be reduced if the stressor level is either lower or higher than ρ_1. This phenomenon, where a stressor improves a desirable response at intermediate levels, is known in toxicology as hormesis and has been observed in bioassay tests with a wide variety of organisms (e.g. Calabrese & Baldwin, 1998). An example of a hormetic stressor in the context of stream integrity is nitrate.

In eqs (6) and (7), we now have a complete model relating stream integrity at stream location x to land cover-related stressor loadings and attenuation rates throughout the catchment. It consists of the following pair of equations:

$$\left.\begin{array}{l}\rho(x) = \sum_{i=1}^{N} \rho(i \rightarrow x) \\ I(x) = f(\rho(x)),\end{array}\right\} \qquad (8)$$

where $\rho(i \rightarrow x)$ is given by eqn (4) or (5). The first eqn in (8) characterises the dependence of the cumulative stressor load on catchment loadings and attenuation rates; the second characterises the dependence of stream integrity on the cumulative stressor load.

Extensions of the model The model developed here includes a number of simplifying assumptions. The approach is flexible, however, and can be extended in various ways. For example, if estimates were available for grid-cell loadings (λ) of specific stressors, such as sediment, nitrogen and phosphorus, these could be incorporated into the model. These loadings could be estimated directly from land cover and land use information for each grid cell, roughly similar to the approach employed on a catchment-aggregated basis by the General Watershed Loading Functions model (Haith & Shoemaker, 1987). Also, current implementation of the model requires that we interpret the grid-cell loadings as unspecified land cover-related influences that are transported through the catchment along hydrologic pathways and exhibit attenuation with transport distance. The model could also be extended to address differences in grid-cell loadings, terrestrial attenuation rates and functional attributes of riparian habitats depending on local topography, physiographic, or hydrologic characteristics (Correll, 2000). Other features that could be incorporated in the model include allowing instream habitat attributes to influence biological metrics, and more generally, allowing stressor–response functions to depend on loads or concentrations of multiple stressors. Finally, explicit sources of variability and uncertainty could be incorporated in the model, making it possible to quantify uncertainty in model predictions.

Application to restoration planning

In this section we apply the model to a set of small Piedmont catchments in the mid-Atlantic region of the eastern U.S. We use geospatial datasets and survey data from stream macroinvertebrate and algal communities to estimate stressor attenuation rates and parameters for stressor–response functions. We then show how the model can be used to guide restoration planning in a case study catchment by predicting the quantitative change in biological characteristics of stream communities resulting from implementation of a hypothetical restoration project.

Study catchments

The model is empirically based, and thus the data used to estimate model parameters is an important consideration for any proposed application. In general, these data should include catchments exhibiting stresses imposed on streams, and stream ecosystem characteristics covering the entire range of conditions over which the model is to be applied. For example, if one wishes to use the model to determine the restoration needs to improve ecosystems to an unimpaired status, then the data used to estimate model parameters must also include catchments where ecosystems are unimpaired. If these data are not available, the model cannot be applied in this way. Similarly, these data should emphasise differences in catchment land cover and stream ecosystem characteristics of concern (i.e. variables considered by the model), but be as similar as possible in all other respects.

Study catchments were selected to represent a range of forested and non-forested land cover conditions, but were similar in terms of physiography, ecoregion and climate. Physiographic and stream-size differences among study sites were minimised by including only first-, second- and small third-order streams on the Piedmont Plateau of southeastern Pennsylvania, northern Delaware and northern Maryland. The Piedmont Plateau in these areas is composed of broad, rolling hills in the Piedmont Uplands and less steep, rolling hills in the Piedmont Lowlands. The Uplands occur mainly on metamorphic schists and related rock, and the Lowlands on sandstone and shale (U.S. Geological Survey, 1997). Soils are primarily alfisols and well developed ultisols (Ciolkosz *et al.*, 1989). The region supports a fragmented, mixed-hardwood deciduous forest with areas cleared for pasture, agriculture, and suburban development. The average annual precipitation in this area is about 1090 mm.

To simplify the initial phase of model development and calibration, we selected study sites with small amounts of urban development. All study catchments except one had from 1% to 8% urban land cover (e.g. commercial or residential). The remaining site had 18% urban land cover. Study sites were also selected with the least amount of row-crop agriculture as possible. Agricultural, urban and meadow land-cover types were combined into a single land cover category (hereafter called agriculture/meadow) to simplify the present analysis. Thus, the results of this study only address the influence of different patterns of forested versus agriculture/meadow land-cover types, although the model can readily be expanded to examine a large number of land-cover types.

A total of 40 stream sampling sites in 33 different catchments were included in the study (Table 1). Paired forest and meadow sites were sampled on five streams, and three locations were sampled along one stream. Forested reaches had mature, relatively undisturbed riparian forest that was at least 30 m wide along both banks. Meadow and agricultural reaches were bordered by habitat consisting of grasses or other small herbaceous vegetation that was at least 30 m wide along both banks. To limit the complexity of the analysis, sites influenced by dams, bridges, ponds, wastewater discharges, cattle grazing, channel/floodplain modification and other site-specific features were excluded.

Geospatial datasets

Land cover within a 200-m buffer of all perennial stream channels was digitised by hand using approximately 1-m resolution aerial photographs (Digital Orthophoto Quadrangles; U.S. Geological Survey, Reston, VA, U.S.A.). Land cover classifications were updated to circa 2001 using 10-m resolution SPOT satellite imagery. Land cover data for all catchment locations outside the 200-m stream buffer were compiled from 30-m resolution Landsat satellite data from the 1992 U.S. National Landcover Dataset (Vogelmann *et al.*, 2001). A seamless, raster land cover dataset was created with a final cell-size of 10×10 m to reflect the greater resolution of hand-digitised data.

Supporting raster data sets quantifying transport distances along the topographic gradient from each location in the catchment to the stream sampling location were generated using ArcGIS software and digital elevation data. Flow pathways were determined using the ArcGIS FLOWDIRECTION function (ESRI ArcGIS). For each study catchment, five individual datasets quantifying transport distances through forested land cover, agriculture/meadow land cover, first-order, second-order and third-order streams were generated using the ArcGIS FLOW-LENGTH function.

Metrics of stream ecosystem integrity

Field sampling was conducted at each of 40 stream sampling locations during September and October, 2001, using U.S. EPA rapid bioassessment protocols for benthic invertebrates, attached algae and fish (Barbour *et al.*, 1999). Sample organisms were identified to the lowest practical taxonomic level (species for algae and usually genus for benthic macroinvertebrates). These data were used to calculate a suite of biological metrics based on benthic inverte-

Table 1 Catchments included to parameterise a spatially explicit model to predict stream ecosystem integrity from land cover data in low-order stream catchments

			Land cover type		
Stream	County, state	Catchment area (km^2)	Forest	Agriculture/meadow	Urban
Beaver Run (forest)	Chester, PA	11.53	0.62	0.34	0.03
Beaver Run (meadow)	Chester, PA	12.91	0.62	0.34	0.03
Birch Run	Chester, PA	16.31	0.51	0.46	0.02
Burrows Run (forest)	New Castle, DE	15.66	0.50	0.42	0.08
Burrows Run (meadow)	New Castle, DE	17.59	0.49	0.43	0.07
Cooks Creek	Bucks, PA	22.29	0.48	0.48	0.03
Culbertson Run	Chester, PA	10.28	0.26	0.67	0.06
Dismal Creek	Delaware, PA	03.91	0.80	0.12	0.08
E. Br. White Clay Creek	Chester, PA	02.21	0.32	0.66	0.01
Grammies Run (forest)	Cecil County, MD	05.26	0.47	0.51	0.02
Grammies Run (meadow)	Cecil County, MD	03.06	0.50	0.48	0.02
Grammies Run (forest)	Cecil County, MD	04.14	0.47	0.51	0.02
Hay Creek	Berks, PA	46.25	0.70	0.27	0.01
Hodgson Run	Chester, PA	08.38	0.28	0.70	0.01
Holland Brook	Hunterdon, NJ	15.02	0.40	0.53	0.06
Indian Creek	Montgomery, PA	14.25	0.13	0.69	0.18
Indian Run	Chester, PA	11.09	0.51	0.47	0.02
Ironstone Creek	Berks, PA	17.06	0.45	0.51	0.04
Leech Run	Chester, PA	11.79	0.14	0.79	0.06
Leech Run	Chester, PA	11.11	0.12	0.81	0.07
McCreary Run	Chester, PA	09.24	0.12	0.86	0.01
Middle Run	New Castle, DE	04.81	0.26	0.64	0.08
Monacacy Creek	Berks, PA	21.80	0.37	0.57	0.03
Morris Run	Bucks, PA	12.73	0.35	0.58	0.07
Owatin Creek	Berks, PA	10.67	0.43	0.55	0.02
Perkiomen Creek	Berks, PA	13.67	0.66	0.32	0.02
Trib. Perkiomen	Berks, PA	10.54	0.58	0.41	0.01
Pigeon Creek	Chester, PA	18.20	0.62	0.32	0.06
Pine Creek of French	Chester, PA	13.92	0.76	0.22	0.01
Pine Creek of Pickering	Chester, PA	11.64	0.43	0.53	0.04
Pine Run	Bucks, PA	12.42	0.30	0.60	0.10
Schmoutz Creek	Bucks, PA	08.25	0.37	0.60	0.02
S. Br. French Creek (forest)	Chester, PA	24.30	0.39	0.56	0.04
S. Br. French Creek (meadow)	Chester, PA	27.31	0.41	0.55	0.04
Stewart Run	Lancaster, PA	15.12	0.17	0.82	0.02
Trib. Brandywine	New Castle, DE	01.08	0.33	0.65	0.02
Tweed Run	Chester, PA	15.74	0.12	0.80	0.08
W. Br. White Clay Creek	Chester, PA	12.78	0.24	0.70	0.06
Ways Run (Meadow)	Chester, PA	06.51	0.31	0.64	0.04
Ways Run (Forest)	Chester, PA	06.47	0.31	0.65	0.04

brates, benthic algae and fish. In addition to biological data, supporting data describing physical habitat in streams and water quality were also collected.

We illustrate our modelling approach by presenting results for four metrics of stream ecosystem integrity that were found to be informative and to exhibit relatively low pairwise statistical correlation: a periphyton pollution-sensitivity metric (Alg_PS) based on the ratio of pollution-sensitive to pollution-tolerant species of algae from eastern North America (as classified by Patrick & Palavage, 1994), the number of benthic insect taxa in the orders Ephemeroptera, Plecoptera and Trichoptera (Inv_EPT) (Barbour *et al.*, 1999), Hilsenhoff's HBI benthic macroinvertebrate pollution-tolerance index (Inv_HBI) (Hilsenhoff, 1987), and the Shannon–Wiener diversity index for benthic macroinvertebrates (Inv_SW) (Pielou, 1975).

Calculating instream stress

Cumulative stress was estimated at each sampling location using eqs (5) and (6) with five distinct attenuation parameters: one each for forest and agriculture/meadow land cover, and one each for first-, second- and third-order streams. Transport distances through each land cover and stream-order class were read from the five supporting data sets described above. As noted previously, the present version of the model does not include a method for directly estimating grid-cell loadings $\lambda(T_{i0})$ from information on land cover and land use. The method we employed is explained in the next section.

Stressor–response function

The form of stressor–response relationship we chose for this case study is a three-parameter sigmoid function. This function can range from quasi-linear to strongly non-linear, and is therefore useful for characterising a wide range of stressor–response relationships. The sigmoid form is justified on theoretical grounds, as this is the pattern typically found in other biological applications of stressor–response functions (U.S. EPA, 1989). Because some measures of ecosystem integrity decrease with increasing stress (e.g. Inv_EPT) while others increase (e.g. Inv_HBI), we employed decreasing and increasing forms of the same function. The decreasing form $f_D(\rho)$ is given by

$$f_D(\rho) = \left(\frac{1}{1 + ae^{bc\rho}}\right)^{1/c}, \tag{9}$$

where ρ is cumulative stress at the catchment outlet and a, b and c are non-negative parameters to be estimated from the data. The increasing form $f_I(\rho)$ is given by

$$f_I(\rho) = 1 - f_D(\rho). \tag{10}$$

Note that the values of both $f_D(\rho)$ and $f_I(\rho)$ lie between 0 and 1 for all values of instream stress ρ. This requires that measures of ecosystem integrity be normalised to lie between 0 and 1 prior to fitting the stressor–response functions, avoiding the need for an additional (fourth) parameter in the stressor–response function. Normalisation of each measure of ecosystem integrity was done by rescaling such that the maximum observed value was equal to 1, and the minimum observed value was equal to 0.

Stressor loadings from each grid-cell in the catchment were determined as follows. In the current version of the model, we interpret the grid-cell loadings as unspecified land cover-related influences that are transported along hydrologic pathways and exhibit attenuation. We treated forest land cover as a reference condition and assigned its initial grid-cell loading a value of 0. We treated agriculture/meadow land cover as an impaired condition and assigned its initial grid-cell loading an arbitrary positive value, which we may call λ_1. All forest terms therefore drop out of the cumulative stress eqn (6), and all remaining (agriculture/meadow) terms contain the same coefficient λ_1, as can be seen from eqn (5). We now divide cumulative stress ρ by λ_1 to obtain relative stress $\hat{\rho} = \rho/\lambda_1$. Finally, we define a new parameter $\hat{b} = b\lambda_1$ in the stressor–response function, which can then be expressed as a function of relative stress $\hat{\rho}$ instead of absolute stress ρ; that is,

$$f_D(\hat{\rho}) = \left(\frac{1}{1 + ae^{\hat{b}c\hat{\rho}}}\right)^{1/c}. \tag{11}$$

Thus, the form of the stressor–response function is unchanged. The net effect of this procedure is that we interpret cumulative stress as relative rather than absolute stress, we set the grid-cell loading for forest to 0 and the grid-cell loading for agriculture/meadow to 1, and we leave the form of the stressor–response function unchanged while modifying our interpretation of parameter b.

Estimating model parameters

The form of the model developed for this case study has a total of eight parameters to be estimated: five stressor attenuation parameters and three stressor–response function parameters. For any choice of values for its eight parameters, the model predicts stream integrity at each sampling location. Given the observed stream integrity at each sampling location, parameter values were chosen to minimise the sum of squared differences between observed and predicted values of stream integrity. This is equivalent to maximising the following objective function:

$$\mathrm{Y}(\boldsymbol{\theta}) = \frac{\sum(\text{Observed Response})^2}{\sum(\text{Observed Response} - \text{Predicted Response})^2},$$

where θ is the vector of eight parameters. Maximisation of $Y(\theta)$ was carried out using a genetic algorithm written in C++. We chose a genetic algorithm due to the relatively large number of parameters and the likelihood of multiple local minima on the error surface (Goldberg, 1989). Genetic algorithms are theoretically and empirically proven to provide a robust search in complex search space (Goldberg, 1989). Each optimisation run consisted of 1500 generations. Convergence of the solution was tested by running the genetic algorithm 100 times for each metric using a range of different values for the initial population size and the probability of mutation.

Model results

Figure 2 shows the best-fit stressor–response functions for each of the four measures of ecosystem integrity. Overall model goodness of fit, as indicated by the R^2 coefficient (i.e. the per cent of total variance explained by the model), was 48%, 51%, 48% and 43% for Alg_PS, Inv_EPT, Inv_HBI and Inv_SW, respectively. Note that none of the fitted stressor–response functions exhibits pronounced non-linearity. This may be a consequence of excluding catchments with moderate to high amounts of row-crop agriculture

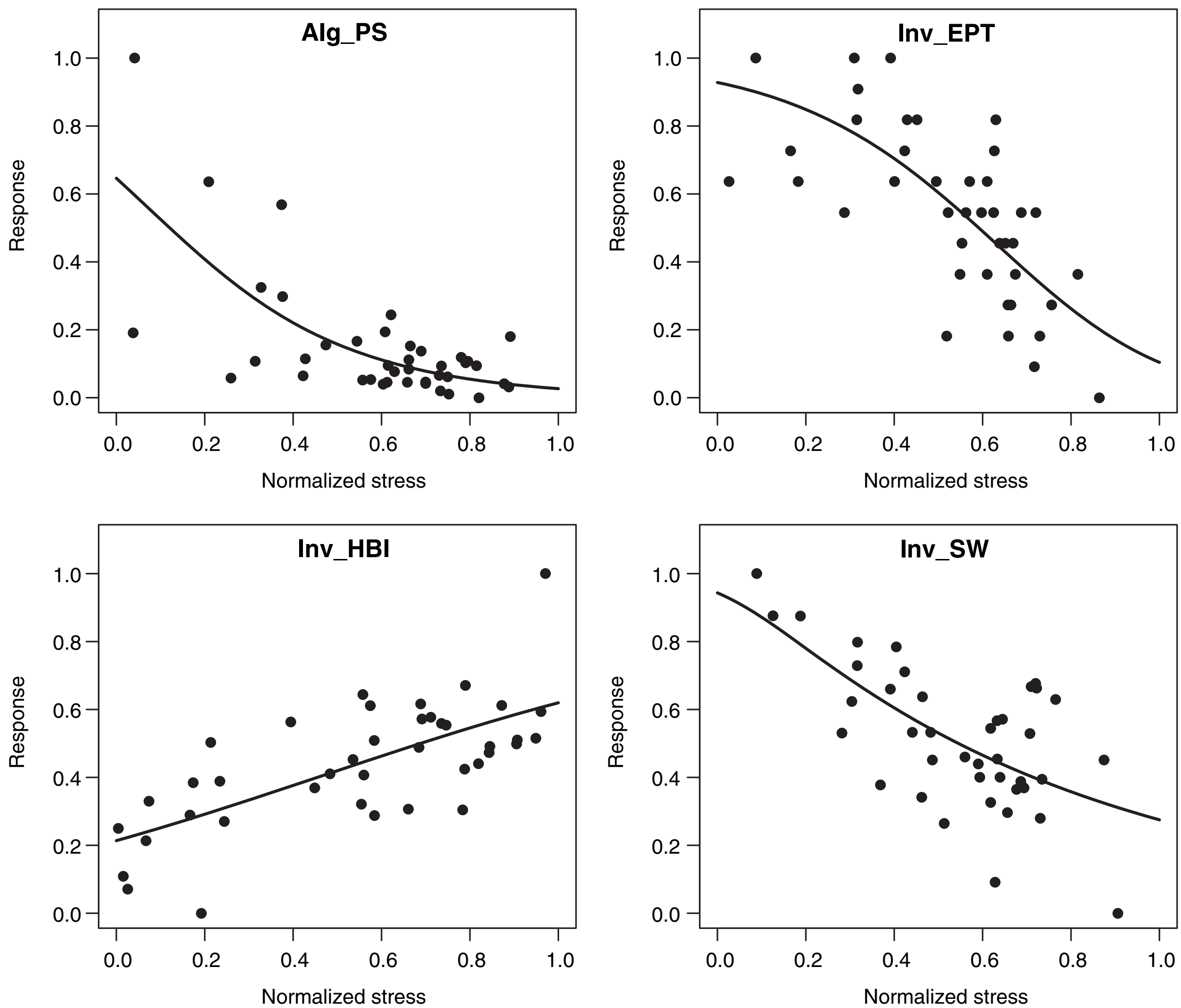

Fig. 2 Fitted stressor–response functions for the four selected metrics of stream ecosystem integrity. Alg_PS: algal pollution-sensitivity index; Inv_EPT: number of benthic insect taxa in orders Ephemeroptera, Plecoptera and Trichoptera; Inv_HBI: Hilsenhoff's Biotic Index of macroinvertebrate pollution tolerance; Inv_SW: Shannon–Weaver diversity index for benthic macroinvertebrates. Square root of the mean squared error (RMSE) and R^2 values are as follows. Alg_PS: RMSE = 0.14, R^2 = 48%; Inv_EPT: RMSE = 0.17, R^2 = 51%; Inv_HBI: RMSE = 0.13, R^2 = 48%; Inv_SW: RMSE = 0.15, R^2 = 43%.

Table 2 Estimated stressor attenuation and parameters of stressor–response functions for each of four metrics to assess stream ecosystem integrity

Parameter	Measure of stream integrity			
	Alg-RP	Inv_EPT	Inv_HBI	Inv_H
Attenuation				
α – Forest	3.5×10^{-3}	2.5×10^{-5}	8.2×10^{-2}	2.1×10^{-3}
α – Non-forest	2.5×10^{-5}	2.8×10^{-4}	6.3×10^{-3}	1.0×10^{-4}
α – First order	4.8×10^{-2}	3.3×10^{-3}	8.4×10^{-3}	6.0×10^{-4}
α – Second order	6.7×10^{-6}	7.5×10^{-4}	2.8×10^{-3}	4.4×10^{-3}
α – Third order	4.4×10^{-4}	4.5×10^{-3}	2.3×10^{-3}	4.9×10^{-3}
Stressor–response				
a	0.99	0.04	0.83	0.79
b	3.62	7.54	1.0	1.31
c	1.59	0.54	2.51	10.0

or urban development, thus compressing the range of cumulative stress levels included in the study set.

Estimated stressor attenuation parameters (α) for the four measures of stream integrity varied over several order of magnitude, from 2.5×10^{-5} to 8.2×10^{-2} m^{-1} for forested land cover and 2.5×10^{-5} to 6.3×10^{-3} m^{-1} for non-forested land cover (Table 2). Differences in instream attenuation parameters were also large, ranging from 6.0×10^{-4} to 4.8×10^{-2} m^{-1} for first-order segments, 6.7×10^{-6} to 4.4×10^{-3} m^{-1} for second-order segments and 4.4×10^{-4} to 4.9×10^{-3} m^{-1} for third-order segments of the stream network.

Although these results show substantial variability, they suggest intuitively plausible solutions for three of the four metrics (Alg-RP, Inv_HBI and Inv_H). In contrast, the higher rate of attenuation for non-forested compared with forested land cover for Inv_EPT suggests this is not a plausible solution. It is not clear why this solution resulted. It is likewise apparent that additional detail is required to refine the solution technique. For example, in the present version of the model, several properties which can influence attenuation are not included. In particular, it is known that the influence of riparian habitats varies in different locations along streams because of differences in hydrologic characteristics (Correll, 2000). The current example does not account for these differences in order to keep presentation of the basic model simple. Other factors such as hillslope gradient and soil characteristics could also be represented in the model, but are not considered here. Parameter estimates from this application should therefore only be considered illustrative of the approach. It should also be noted that no constraints other than non-negativity were imposed on parameter values. If a range of physically plausible values for attenuation parameters were known, or the relative values of parameters could be assumed (e.g. forest attenuation rate never less than non-forest attenuation rate), this constraint could easily be accommodated by the model.

Comparison with a spatially aggregated regression model

For comparison, the three-parameter stressor–response function was also fitted to each of the four measures of ecosystem integrity using whole-catchment percent non-forested land cover as the stress. This is analogous to the special case of the spatially explicit model where all stressor attenuation rates are zero, and the stress at each stream location is influenced equally by land cover in all catchment locations contributing to that point. The resulting R^2 values for these fits were 2%, 19%, 6% and 2% for Alg_PS, Inv_EPT, Inv_HBI and Inv_SW, respectively. In each case, the spatially explicit model explained more than twice the variance explained by the corresponding spatially aggregated model. This indicates that the spatially explicit approach developed here can provide a significantly improved capability for relating catchment land cover to instream ecosystem characteristics, although it does this at the expense of five additional parameters. In our view, the most important advantage purchased by these additional parameters is not the increase in R^2 but the ability of the spatially explicit approach to relate stream ecosystem integrity to the land cover of specific grid cells.

The R^2 values in the whole-catchment fits are also low relative to R^2 values sometimes reported in studies relating urban or agricultural land cover to stream ecosystem characteristics (Scheuler, 1995; Allan, Erickson & Fay, 1997; Fitzpatrick *et al.*, 2001). This result probably reflects the fact that catchments with high amounts of urban land cover and high degrees of associated stream impairment were not included in the data set for this study. Because R^2 is determined not only by the difference between observed and predicted values (i.e. strict goodness of fit) but also by the steepness of the trend underlying the observed values, we suspect that R^2 values would have been higher for both our whole-catchment analysis and our spatially explicit analysis if the dataset had included catchments that were substantially more urbanised.

Predicting restoration outcomes

Using parameter estimates from the mid-Atlantic streams sampled, we now present a quantitative example of how the parameterised model can be used to guide restoration planning. We focus on the McCreary Run catchment, which is one of the 33 catchments used to estimate parameters as discussed above.

Many states in the U.S. designate stream impairment using criteria such as the HBI. Such measures therefore provide a logical way to set restoration goals. For example, suppose managers of the McCreary Run catchment aim at increasing the value of the HBI at the catchment outlet to a specific target value, and that they have selected riparian reforestation at an upstream location as the means for achieving this goal. The problem is to determine the project size (area) that would be required to achieve their HBI goal and they can use the model to assess various restoration scenarios.

Once model parameters have been estimated, the outcome of a proposed riparian restoration project can be predicted by simply changing land cover assignments (using a GIS) for each grid cell that would be restored, recalculating cumulative stress at the evaluation point (the catchment outlet, in this case) based on the new land cover assignments, and then using the stressor–response function to calculate the predicted response of the relevant ecological metric.

When applying the model in this way to predict restoration outcomes, several items should be noted. First, we do not know the 'true' cumulative stress at the McCreary Run catchment outlet prior to restoration, so we use the stress calculated by the model as our best estimate. Secondly, we also do not know the 'true' value of the HBI metric for the McCreary Run catchment outlet prior to restoration. Our estimation procedure assumes that the best estimate of the metric is not the observed value (which includes an error component because of sampling error and temporal variability) but the estimate produced by the model. We therefore use the HBI value calculated by the model to represent the 'before restoration' condition. Thirdly, we employ the recalculated value of the HBI metric after changing land cover assignments as the predicted outcome of a restoration project, although we recognise there is uncertainty in the actual outcome (the important issue of prediction uncertainty is discussed in the next section). Finally, we should point out that the predicted responses of stream communities are expected to materialise only after the maturation of the restored forest habitat, which may require many years. Nevertheless, in the context of restoration planning, knowledge of the likely long-term ecosystem response to restoration provides an effective method for designing, siting and prioritising projects.

Figure 3 shows the stressor–response function for HBI for benthic macroinvertebrates as obtained by fitting the model described above to the McCreary Run catchment (Fig. 4). The point labelled 'Before' in Fig. 3 is the estimated true level of stress imposed on the stream (horizontal axis) and the response of its macroinvertebrate community (vertical axis) before restoration. The dashed horizontal line labelled 'Target' indicates the HBI value to be achieved. The

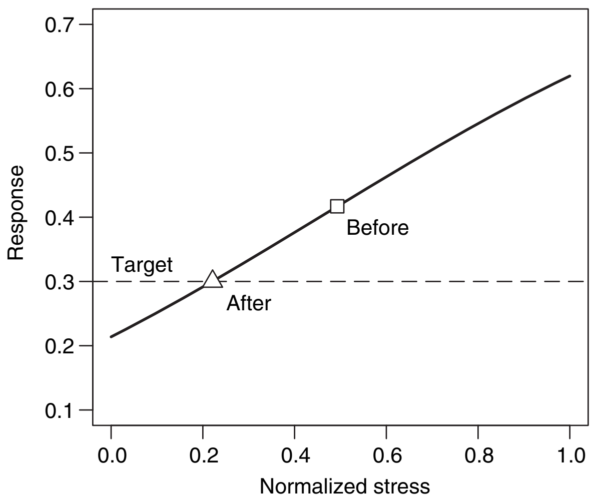

Fig. 3 The response of stream ecosystem integrity (as measured by Hilsenhoff's Biotic Index, HBI) to cumulative stress at the outlet of the McCreary Run catchment. The curve shown is the fitted stressor–response function. The point labelled 'Before' indicates the best model estimate of stream ecosystem integrity at the catchment outlet and the associated level of (normalised) stress when data were collected (i.e. before restoration). The dashed horizontal line labelled 'Target' indicates the HBI value to be achieved. The point labelled 'After' indicates the best model estimate of stream ecosystem integrity after restoration; the amount of restoration was chosen so that this value coincides with the target.

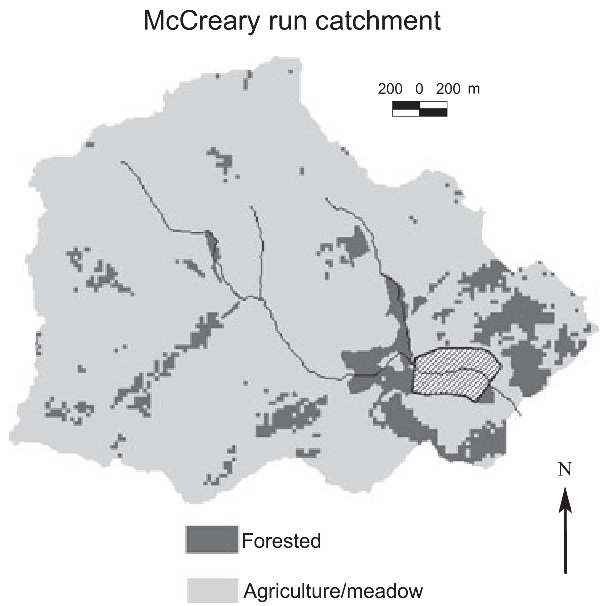

Fig. 4 The McCreary Run catchment of southeastern Pennsylvania, U.S.A., showing the spatial distribution of forest and non-forest land-cover types. The hatched area shows the extent of a hypothetical riparian restoration project.

hatched area in Fig. 4 shows a hypothetical restoration project in which riparian agriculture/meadow land cover is changed to forest, with the area of habitat restored being just sufficient to increase the predicted value of HBI (the point labelled 'After' in Fig. 3) to the target level. The predicted outcome of the project was determined by changing the land-cover type in the indicated area from agriculture/meadow to forest in a GIS and then using the fitted model to recalculate HBI. In the same manner, the fitted model can be used to predict the likely outcomes of a variety of alternative restoration projects in any catchment appropriately similar to those catchments used to estimate model parameters (i.e. in size, physiography, ecoregion, climate, etc.).

Conclusions and outlook

In this paper we develop and apply a spatially explicit, empirically based model that quantitatively links the spatial pattern of catchment land cover to specific measures of stream ecosystem integrity. With continued development, the model has the potential to serve as a powerful planning tool for estimating the width, extent and location of riparian reforestation needed to restore desired ecosystem characteristics in streams impaired by land cover-related stresses such as sediment and nutrient loading. At present, there are very few quantitative tools available to restoration practitioners that can help them plan and implement projects in a way that maximises their catchment-level benefits. A simple version of the model is presented here that illustrates the conceptual basis of the approach.

The results of this work suggest a number of ways the model could be further developed and improved. Potentially important factors not addressed in the current form of the model include differences in riparian function associated with hydrologic characteristics at different locations along the stream, accounting for additional land-cover types such as urban and row-crop agriculture, and accounting for multiple stressors simultaneously. The current model could be extended to account for each of these factors.

In addition, an approach for dealing with model uncertainty is desirable prior to applying the model. As noted previously, the present version of the model does not incorporate explicit sources of variability or uncertainty and therefore does not address their consequences. Inevitably, however, there will be significant variability in stressor loadings from each land-cover type (e.g. the same land-cover type in different catchments or years) and in stream ecosystem characteristics at different times. These sources of variability create uncertainty in estimated parameter values and subsequent model predictions. The extent of uncertainty in model predictions can best be addressed by explicitly propagating parameter uncertainties through the model to determine the resulting probability distributions of predicted outcomes. Using this approach, it will be possible to estimate, for example, the amount of riparian restoration which yields a 95% probability that stream ecosystem integrity (as judged by a particular metric) will be increased to the target value or better. Work is currently underway to develop a method for conducting such probabilistic analyses based on bootstrapping.

This work suggests the potential usefulness of spatially explicit, empirically calibrated models in predicting the catchment-level benefits of riparian restoration projects. With additional development, this type of model may also hold promise for addressing a variety of additional catchment management problems (Power *et al.*, 2005).

Acknowledgments

We are grateful to Richard Horwitz, Rebecca Brown and Jim Thomson at the Academy of Natural Sciences, Patrick Center for Environmental Research for early reviews of this manuscript. We are also indebted to our colleagues at the Patrick Center: Jamie Carr, Don Charles, Tim Nightengale, Karen Rowley, David Velinsky and Diane Winter who contributed generously to the field sampling, GIS analysis and general development of the ideas presented in this paper. Finally, we very much appreciate the efforts of Roland Jansson and Mark Gessner that made this special issue possible, and for the many thoughtful and constructive comments provided by three anonymous reviewers of this manuscript. This research was supported by the Pennsylvania Department of Environmental Protection, the William Penn Foundation and the Patrick Center's Endowment for Innovative Research. The views expressed herein are those of the authors and do not necessarily reflect the views of the Pennsylvania Department of Environmental Protection or William Penn Foundation.

References

Alexander R.B., Smith R.A. & Schwarz G. (2000) Effect of stream channel size on the delivery of nitrogen to the Gulf of Mexico. *Nature*, **403**, 758–761.

Allan J.D (1995) *Stream Ecology: Structure and Function of Running Waters*. Chapman & Hall, London, U.K.

Allan J.D. (2004) Landscapes and riverscapes: the influence of land use on stream ecosystems. *Annual Review of Ecology, Evolution and Systematics*, **35**, 257–284.

Allan J.D., Erickson D.L. & Fay J. (1997) The influence of catchment land use on stream integrity across multiple spatial scales. *Freshwater Biology*, **37**, 149–161.

Altier L.S., Lowrance R., Williams R.G., Inamdar S.P., Bosch D.D., Sheridan J.M., Hubbard R.K. & Thomas D.L. (2002) *Riparian Ecosystem Management Model: Simulator for Ecological Processes in Riparian Zones*. Conservation Research Report 46. USDA, ARS, Tifton, GA, U.S.A.

Amoros C. & Bornette G. (2002) Connectivity and biocomplexity in waterbodies of riverine floodplains. *Freshwater Biology*, **47**, 761–776.

Barbour M.T., Gerritsen J., Snyder B.D. & Stribling J.B. (1999) *Rapid Bioassessment Protocols for Use in Streams and Wadeable Rivers: Periphyton, Benthic Macroinvertebrates, and Fish*, Second Edition. EPA 841-B-99-002. U.S. Environmental Protection Agency, Office of Water, Washington, DC, U.S.A.

Bell S.S., Fonseca M.S. & Motten L.B. (1997) Linking restoration and landscape ecology. *Restoration Ecology*, **5**, 318–323.

Bernhardt E.S., Palmer M.A., Allan J.D. *et al.* (2005) Synthesizing U.S. River Restoration. *Science*, **308**, 636–637.

Bohn B.A. & Kershner J.L. (2002) Establishing aquatic restoration priorities using a catchment approach. *Journal of Environmental Management*, **64**, 355–363.

Calabrese E.J. & Baldwin L.A. (1998) Hormesis as a biological hypothesis. *Environmental Health Perspectives*, **106**, 357–362.

Ciolkosz E.J., Waltman W.J., Simpson T.W. & Dobos R.R. (1989) Distribution and genesis of soils of the northeastern United States. *Geomorphology*, **2**, 285–302.

Correll D.L. (2000) The current status of our knowledge of riparian buffer water quality functions. In: *Proceedings of International Conference on Riparian Ecology and Management in Multi-Land use Catchments* (Eds P.J. Wigington & R.L. Beschta), pp. 5–10. American Water Resources Association, Middleburg, VA, U.S.A.

Dale-Jones E.B. III, Helfman G.S., Harper J.O. & Bolstad P.V. (1999) Effects of riparian forest removal on fish assemblages in southern Appalachian streams. *Conservation Biology*, **13**, 1454–1465.

Endreny T.A. & Wood E.F. (2003) Catchment weighting of export coefficients to map critical phosphorus loading areas. *Journal of the American Water Resources Association*, **39**, 165–180.

Fitzpatrick F.A., Scudder B.C., Lenz B.N. & Sullivan D.J. (2001) Effects of multi-scale environmental characteristics on agricultural stream biota in eastern Wisconsin. *Journal of the American Water Resources Association*, **37**, 1489–1507.

Goldberg D.E. (1989) *Genetic Algorithms in Searching, Optimization, and Machine Learning*. Addison Wesley, Reading, MA, U.S.A.

Gomi T., Sidle R. & Richardson J. (2002) Understanding processes and downstream linkages of headwater systems. *BioScience*, **52**, 905–916.

Gove N.E., Edwards R.T. & Conquest L.L. (2001) Effects of scale on land use and water quality relationships: a longitudinal basin-wide perspective. *Journal of the American Water Resources Association*, **37**, 1721–1734.

Gregory S.V., Swanson F.J., McKee A. & Cummins K.W. (1991) Ecosystem perspectives of riparian zones. *BioScience*, **41**, 540–551.

Haith D.A. & Shoemaker L.L. (1987) Generalized watershed loading functions for stream flow nutrients. *Water Resources Bulletin*, **23**, 471–478.

Harris G. (2002) *Simple Rules underlie the Complex and Non-linear Dynamics of Terrestrial and Aquatic Ecosystems: Implications for Catchment Biogeochemistry and Modeling*. Technical Report 11/02, April 2002, CSIRO Land and Water, Dickson ACT, Australia.

Hilsenhoff W.L. (1987) An improved biotic index of organic stream pollution. *The Great Lakes Entomologist*, **20**, 31—39.

Hynes H.B.N. (1975) The stream and its valley. *Verhandlungen der Internationalen Vereinigung für Theoretische und Angewandte Limnologie*, **19**, 1–15.

Jones K.B., Neale A.C., Nash M.S., Van Remortel R.D., Wickham J.D., Riitters K.H. & O'Neill R.V. (2001) Predicting nutrient and sediment loadings to streams from landscape metrics: a multiple catchment study from the United States Mid-Atlantic Region. *Landscape Ecology*, **16**, 301–312.

Junk W.J., Bayley P.B. & Sparks R.E. (1989) The flood pulse concept in river floodplain systems. *Special Publication Canadian Journal of Fisheries and Aquatic Sciences*, **106**, 110–127.

Lowrance R.R., Altier L.S., Williams R.G., Imamdar S.P., Bosch D.D., Hubbard R.K. & Thomas D.L. (2000) The riparian ecosystem management model. *Journal of Soil and Water Conservation*, **55**, 27–36.

Montgomery D.R. & Buffington J.M. (1993) *Channel Classification, Prediction of Channel Response, and Assessment of Channel Condition*. Washington State Department of Natural Resources Report TFW-SH10-93-002.

Moser T.J., Lindeman D.R., Wigington P.J., Schuft M.J. & van Sickle J. (2000) Methods for multi-spatial scale characterization of riparian corridors. In: *Proceedings of International Conference on Riparian Ecology and Management in Multi-Use Watersheds* (Eds P.J. Wigington & R.L. Beschta), pp. 511–516. American Water Resources Association, Middleburg, VA, U.S.A.

National Research Council (NRC) (2002) *Riparian Areas: Functions and Strategies for Management*. Committee on Riparian Areas Function and Strategies for Management, National Academy Press, Washington, DC, U.S.A.

Patrick R. & Palavage D.M. (1994) The value of species as indicators of water quality. *Proceedings of the Academy of Natural Sciences of Philadelphia*, **145**, 55–92.

Pielou E.C. (1975) *Ecological Diversity*. John Wiley, New York.

Power M.E., Brozovi N., Bode C. & Zilberman D. (2005) Spatially explicit tools for understanding and sustaining inland water ecosystems. *Frontiers in Ecology and the Environment*, **3**, 47–55.

Preston S.D. & Brakebill J.W. (1999) *Application of Spatially Referenced Regression Modeling for the Evaluation of Total Nitrogen Loading in the Chesapeake Bay Catchment*. USGS Water Resources Investigations Report 99-4054.

Scheuler T.R. (1995) The importance of imperviousness. *Watershed Protection Techniques*, **1**, 100–111.

Smith R.A., Schwarz G.E. & Alexander R.B. (1997) Regional interpretation of water-quality monitoring data. *Water Resources Research*, **33**, 2781–2798.

Sponseller R.A., Benfield E.F. & Valett H.M. (2001) Relationships between land use, spatial scale and stream macroinvertebrate communities. *Freshwater Biology*, **46**, 1409–1424.

Strayer D.L., Beighley R.E., Thompson L.C., Brooks S., Nilsson C., Pinay G. & Naiman R.J. (2003) Effects of land cover on stream ecosystems: roles of empirical models and scaling issues. *Ecosystems*, **6**, 407–423.

Stream Solute Workshop (1990) Solute dynamics in streams. *Journal of the North American Benthological Society*, **9**, 95–119.

Sweeney B.W. (1992) Streamside forests and the physical, chemical, and trophic characteristics of piedmont streams in eastern North America. *Water Science and Technology*, **26**, 2653–2673.

Tabacchi E., Correll D.L., Hauer R., Pinay G., Planty-Tabacchi A.M. & Wissmar R.C. (1998) Development, maintenance, and role of riparian vegetation in the river landscape. *Freshwater Biology*, **40**, 497–516.

U.S. Environmental Protection Agency (EPA) (1989) *Short-term Methods for Estimating the Chronic Toxicity of Effluents and Receiving Waters to Freshwater Organisms*. EPA/600/4-89/001.

U.S. Environmental Protection Agency (EPA) (1998) *Guidelines for Ecological Risk Assessment*, *U.S*. Environmental Protection Agency, Office of Research and Development, EPA/630/R-95/002F.

U.S. Geological Survey (1997) *Ground Water Atlas of the United States – Segment 11: Delaware, Maryland, New Jersey, North Carolina, Pennsylvania, Virginia, West Virginia*. U.S. Geological Survey Hydrologic Investigations Atlas 730-L, Reston, VA, U.S.A.

Vogelmann J.E., Howard S.M., Yang L., Larson C.R., Wylie B.K. & Van Driel N. (2001) Completion of the 1990s national land cover data set for the conterminous United States from Landsat Thematic Mapper data and ancillary data sources. *Photogrammetric Engineering and Remote Sensing*, **67**, 650–662.

Ward J.V., Tockner K., Arscott D.B. & Claret C. (2002) Riverine landscape diversity. *Freshwater Biology*, **47**, 517–539.

Weller D.E., Jordan T.E. & Correll D.L. (1998) Heuristic models for material discharge from landscapes with riparian buffers. *Ecological Applications*, **8**, 1156–1169.

Welsch D. (1991) *Riparian Forest Buffers: Function and Design for Protection and Enhancement of Water Resources*. USDA Forest Service, Pub. No. NA-PR-07-91.

Wissmar R.C. & Beschta R.L. (1998) Restoration and management of riparian ecosystems: a catchment perspective. *Freshwater Biology*, **40**, 571–585.

Yuan L.L. & Norton S.B. (2003) Comparing responses of macroinvertebrate metrics to increasing stress. *Journal of the North American Benthological Society*, **22**, 308–322.

(Manuscript accepted 21 November 2006)